Archive of Applied Mechanics 71 (2001) 509 – 524 © Springer-Verlag 2001

Accurate modelling of piezoelectric plates: single-layered plate

A. Fernandes, J. Pouget

Summary The paper presents an efficient two-dimensional approach to piezoelectric plates in the framework of linear theory of piezoelectricity. The approximation of the through-the-thickness variations accounts for the shear effects and a refinement of the electric potential. Using a variational formalism, electromechanically coupled plate equations are obtained for the generalized stress resultants as well as for the generalized electric inductions. The latter are deduced from the conservative electric charge equation, which plays a crucial role in the present model. Emphasis is placed on the boundary conditions at the plate faces. The model is used to examine some problems for cylindrical bending of a single simply supported plate. Number of situations are examined for a piezoelectric plate subject to (i) an applied electric potential, (ii) a surface density of force, and (iii) a surface density of electric charge. The through-thickness distributions of electromechanical quantities (displacements, stresses, electric potential and displacement) are obtained, and compared with results provided by finite element simulations and by a simplified plate model without shear effects. A good agreement is observed between the results coming from the present plate model and finite element computations, which ascertains the effectiveness of the proposed approach to piezoelectric plates.

Keywords Piezoelectricity, Plate, Variational Formulation, Finite element method

1 Introduction

The important economic and technical developments of piezoelectricity have attracted much attention in the research of theoretical and computational models of *piezoelectric composites*. Among interesting materials capable of being viable candidates for actuators or sensors, piezoelectric materials have received the most attention, [1]. One of the key factors for this choice is that piezoelectric materials act either as *actuators* or as *sensors*, and relate electric signals directly to material strains or stresses, and vice versa. Piezoelectric materials, and especially piezoelectric composites, are used for multi-purpose devices or smart materials, and numerous technological applications have been proposed, running from aerospace structures (shape control of large space antennas, active control of vibrations), [2, 3], to miniature medical apparatus (micro-robots, pumps, micro-positioning devices), [4]. Nevertheless, producing practically meaningful actuation or sensing capabilities with piezoelectric materials should be included into structures, in the form of *laminated plates*, e.g. bimorphs, piezoelectric layers joined to nonpiezoelectric slabs, sandwich structures or even embedded piezoelectric patches in elastic materials. A great deal of attention should be given to piezoelectric plates as basic components of multi-layered structures. In the present work, special attention is devoted to *single piezoelectric plate* formulation.

Although quite a number of recent studies have shown considerable progress toward establishing correct and efficient plate models along with corresponding equations, better modelling of the electromechanical field through-the-thickness distribution becomes necessary

Received 17 July 2000; accepted for publication 26 September 2000

A. Fernandes, J. Pouget (✉)
Laboratoire de Modélisation en Mécanique (UMR 7607),
Université Pierre et Marie Curie, Case 162,
4 Place Jussieu, F-75252 Paris Cedex 05, France
e-mail: jop@ccr.jussieu.fr

in engineering. The objective of the present work is twofold: (i) to construct an accurate model based on *approximations of the elastic displacements and electric potential* as functions of the thickness coordinate of the plate, and (ii) to assess the *capability of the model* to describe the global plate response, local variations of both mechanical and electric variables, stresses, as well as the limitations of the model. We propose here an efficient plate model which accounts for *shearing effects* of the "sine" type, satisfying the condition of vanishing shear stress at the faces of the plate, [5]. Our piezoelectric plate approach is valid for all kinds of electromechanical loads (surface density of force, electric potential or charges).

The present version of plate model is quite complete in comparison to the most piezoelectric plate models considering only applied electric potential as load. A significant number of works have been devoted to piezoelectric plates, attempting to incorporate various through-the-thickness approximations of laminated piezoelectric beams, plates and shells, [6]. One of the first piezoelectric plate approaches was given in [7], followed by [8] and [9]. The simplest model is based on the kinematic assumptions of Love's first approximation, including the electric degree of freedom. Mindlin [8] has considered an expansion of the elastic displacements and electric potential as polynomial functions, the level of truncation of the expansion leading to the order of the plate theory. Governing plate equations [10] were derived using the kinematic of the first-order shear deformation theory assumption developed by Reissner and Mindlin for purely elastic plates. Some formulations of piezoelectric plates assume, *a priori*, that the normal component of the electric displacement is constant through the thickness, [11]. As a consequence, the conservation law for electric charge or the Gauss equation drops out. It turns out that such an assumption is not satisfied in most situations, and we must consider the approximation of the *electric charge equation*. Due to the limitations of the standard plate theory, it seems to be necessary to investigate a more refined and efficient approach to piezoelectric plates.

In the present study, we attempt to develop a consistent approach to piezoelectric plates based on approximate equations deduced from a generalized variational formulation. The latter involves electromechanical loads prescribed in a natural way on the plate boundary. From the variational formulation are obtained equations for the generalized stress and electric charge or induction resultants. The final set of two-dimensional effective equations governs the extensional (or membrane), flexural and shear deformations, coupled to the applied and induced electric potential. Various benchmark tests are then proposed in order to validate the present approach. Especially, different situations with particular electromechanical loads are regarded: (i) *density of applied forces*, (ii) *applied electric potential* on the top and bottom faces of the plate, and (iii) *applied surface density of electric charges* on both faces of the plate.

In order to draw attention to the capabilities of the model, some comparisons to *finite element* (FE) *computations* for identical situations in 3D problems are proposed. In addition, the results are compared to those coming from the classical plate model based on Love's first approximation (lacking shear effects). The practical example is the *cylindrical bending of a simply supported piezoelectric plate*, for which solutions to the plate equations are looked for in form of Fourier series.

The prerequisites of the piezoelectric formulation (the variational principle, equations of conservation and constitutive laws) are briefly stated in the next section. The through-the-thickness approximation of elastic displacements and electric potential is presented in Sec. 3, together with some comments. The equations for the two-dimensional approach to a piezoelectric plate as well as the associated mechanical and electric boundary conditions are presented in Sec. 4. The problem of a single piezoelectric plate under cylindrical bending is given in Sec. 5 in the cases of an applied electric charge and applied electric potential. In Sec. 6, the numerical results for different kinds of electromechanical loads and slenderness ratios are discussed. The results are also compared to those provided by the FE simulations and by an elementary plate model. Finally, Sec. 7 is devoted to the discussion of the results and extensions of the model to piezoelectric laminated plates.

2
Formulation of piezoelectricity

In this section, we briefly recall the necessary ingredients of linear piezoelectricity and the associated variational formulation based on the *Hamilton's principle*. Assuming that the deformations are infinitesimal, and the electric field is small enough, and there are no body forces, the Hamilton's principle can be stated as follows:

$$\delta \int_{t_1}^{t_2} \int_{\Omega} \mathscr{L} \, \mathrm{d}v \, \mathrm{d}t + \int_{t_1}^{t_2} \delta W \, \mathrm{d}t = 0 \quad . \tag{1}$$

Here, the Lagrangian functional is given by

$$\mathscr{L} = \frac{1}{2} \rho \dot{u}_i \dot{u}_i - H(S_{ij}, E_i) \quad , \tag{2}$$

where $\dot{u}_i$ is the displacement component, ρ is the mass density, $H(S_{ij}, E_i)$ is the electric enthalpy density function, $S_{ij} = u_{(i,j)} = 1/2(u_{i,j} + u_{j,i})$ is the linear part of the strain tensor component and E_i is the electric field vector. For the linear piezoelectricity, the enthalpy density function takes on the form, [12],

$$H(S_{ij}, E_i) = \frac{1}{2} \sigma_{ij} S_{ij} - \frac{1}{2} D_i E_i \quad . \tag{3}$$

Here, σ_{ij} and D_i represent the components of the stress tensor and the electric displacement vector, respectively. Furthermore, the virtual work of the prescribed mechanical and electric quantities on the domain boundary is given in Eq. (1) by

$$\delta W = \int_{\partial\Omega} T_i \delta u_i \, \mathrm{d}S + \int_{\partial\Omega} Q \delta\phi \, \mathrm{d}S \quad . \tag{4}$$

The virtual work involves the surface traction vector **T** and applied surface density of electric charge Q on the boundary $\partial\Omega$. The quantity ϕ is the electric potential. A further step in the simplification can be made by assuming a *quasi electrostatic approximation*, which allows for the electric field to be derived from the electric potential

$$E_i = -\phi_{,i} \quad . \tag{5}$$

It is also supposed that the piezoelectric material is a perfect isolator (no volumic electric charges) and that the magnetic field and magnetization have no influence. Using the integration by parts and assuming the variations δu_i and $\delta\phi$ are arbitrary throughout the domain Ω, the field equations in Ω are

$$\sigma_{ij,j} = \rho \ddot{u}_i, \quad D_{i,i} = 0 \quad . \tag{6}$$

The associated boundary conditions read

$$\sigma_{ij} n_j = T_i \quad \text{or} \quad u_i = \bar{u}_i \quad \text{on } \partial\Omega, \quad D_i n_i = Q \quad \text{or} \quad \phi = \bar{\phi} \quad \text{on } \partial\Omega \quad . \tag{7}$$

The field equations are completed by the constitutive equations. The latter can be deduced for the linear piezoelectricity from the following form for the enthalpy density function, [12]:

$$H(S_{ij}, E_i) = \frac{1}{2} C^E_{ijpq} S_{ij} S_{pq} - e_{ipq} E_i S_{pq} - \frac{1}{2} \epsilon^S_{ij} E_i E_j \quad , \tag{8}$$

where C^E_{ijpq}, e_{ipq} and ϵ^S_{ij} are the elastic, piezoelectric and dielectric permittivity constants, respectively. Accordingly, the constitutive laws for linear piezoelectricity are

$$\sigma_{ij} = \frac{\partial H}{\partial S_{ij}} = C^E_{ijpq} S_{pq} - e_{lij} E_l, \quad D_i = -\frac{\partial H}{\partial E_i} = e_{ipq} S_{pq} + \epsilon^S_{ij} E_j \quad . \tag{9}$$

The set of Eqs. (5)–(7) and (9) are the essentially basic equations of linear piezoelectricity, which are going to be used in the following.

3
The plate approximation for displacement field and electric potential

An expansion of the displacement in power series of the thickness coordinate is commonly considered in the plate theory. Different refined models can be introduced according to the form of the expansion approximation. Other approaches to plates are based on an asymptotic theory of the full 3D problem, [13]. In the present work, the displacement field and electric potential are assumed to be of the form

$$\begin{aligned} u_\alpha(x,y,z,t) &= U_\alpha(x,y,t) - zw_{,\alpha}(x,y,t) + f(z)\gamma_\alpha(x,y,t), \quad \alpha \in \{1,2\}, \\ u_3(x,y,z,t) &= w(x,y,t), \\ \phi(x,y,z,t) &= \phi_0(x,y,t) + z\phi_1(x,y,t) + P(z)\phi_2(x,y,t) + g(z)\phi_3(x,y,t) \ . \end{aligned} \tag{10}$$

It is important to discuss the above expansion in detail.

(i) In the case of purely elastic media, if $f(z) = 0$, we recover the classical theory of Love-Kirchhoff for elastic thin plates, [14]. Particular forms of the function $f(z)$ give rise to different models which have been investigated by Reissner, [15], Ambartsumian, [16] and Reddy, [17], to quote just the most known approaches. In Eq. $(10)_1$ U_α represents the *middle plane displacement components*, w the *deflection* and γ_α is associated with the *shearing effects*. The subscript α takes the value 1 or 2. All the functions are defined at the middle plane coordinate $(x,y,0)$. In the present model, the through-thickness distribution of the shearing effect is approximated by a *trigonometric function*.

(ii) Insofar as the electric potential is concerned, the first two terms in Eq. (10) (linear part) hold for the influence of the *applied electric potential* on the plate faces. The third term can be referred to as the *induced electric potential* by the elastic deformation mediated by the *piezoelectric coupling*. The last term is due to the shearing effect through the piezoelectric coupling. As a consequence, we adopt the following functions:

$$f(z) = \frac{h}{\pi}\sin\left(\frac{\pi z}{h}\right), \quad g(z) = \frac{h}{\pi}\cos\left(\frac{\pi z}{h}\right), \quad P(z) = z^2 - \left(\frac{h}{2}\right)^2 \ , \tag{11}$$

where h is the plate thickness which is supposed to be uniform. The case of the purely elastic plates has been examined in [5] for single and multi-layered plates. Extension to elastic shells has been also considered, [18]. In the classical theory of piezoelectric plates, the shearing effect is removed and the second-order term in the approximation of the electric potential is often neglected. Nevertheless, most applications of the piezoelectric adaptive plates are based mainly on the first-order shear deformation assumption, [10]. We are going to see the implications of the present approximation in the plate equations.

Three kinds of electromechanical conditions are considered on the plate boundaries:

(a) The plate is loaded by a *force density per unit area* on the top face of the plate and perpendicular to this face.

(b) An *applied electric potential* on the top and bottom faces of the plate is considered such as

$$\phi(x,y,z=\pm h/2,t) = V^{\pm}(x,y,t) \ . \tag{12}$$

From Eq. (11), we note that $P(\pm h/2) = 0$ and $g(\pm h/2) = 0$. Then, we deduce that

$$\phi_0 = \frac{1}{2}(V^+ + V^-) \quad \text{and} \quad \phi_1 = \frac{1}{h}(V^+ - V^-) \ . \tag{13}$$

Accordingly, the unknown functions ϕ_0 and ϕ_1 are no longer arbitrary, and they depend on the applied electric potential. For practical cases, it is more convenient to take $V^+ = +V$ and $V^- = -V$, so that we have $\phi_0 = 0$ and $\phi_1 = 2V/h$.

(c) Another possible electric boundary condition are *electric charges* imposed on the top and bottom faces of the plates. In this situation, the electric boundary condition on the electric displacement is given by

$$[\![\mathbf{D}]\!] \cdot \mathbf{n} = q \ ,$$

where $\mathbf{n}$ is the unit outward normal vector to the boundary and q is the surface density of electric charge. In the case of a plate geometry, the condition reads as

$$D_3(x, y, z = \pm h/2, t) = q(x, y, t) \ . \tag{14}$$

We should underline the boundary conditions associated with the electric field. The boundary condition deduced from the formulation of the Maxwell equations reads as $[\![\mathbf{E}]\!] \times \mathbf{n} = 0$, which means that the tangential components of the electric field must be continuous through the interface, [19]. In order to apply an electric potential to the plate faces, the latter are coated with thin metallic electrodes of negligible thickness and playing no role mechanically. Moreover, it is assumed that the stresses and displacements are perfectly transmitted through the electrodes. Since in a conductor the electric field is zero (or the electric potential is constant), the boundary condition on the electric field can be written as $E_1 = E_2 = 0$ on the top and bottom faces of the piezoelectric plate.

It is worthwhile specifying that the surface density of the electric charge $-q$ is applied on the bottom face, while we have $+q$ on the top. Then, the boundary condition on the electric displacement is $-D_3 = -q$ at $z = -h/2$ and $D_3 = +q$ at $z = +h/2$, whence Eq. (14).

4 Plate equations

Plate equations are deduced by using the variational formulation presented in Sec. 2. By taking the approximation of the displacement field and electric potential as defined by Eq. (10), the dependence of the field (u_1, u_2, u_3, ϕ) upon the thickness coordinate z can be cancelled out by integrating over the plate thickness. The procedure leads, in a natural way, to the definition of the generalized stresses and electric charges or inductions. More precisely, the equations of motion and the associated boundary conditions are obtained by, first, substituting the approximation (10) into the variational principle (1)–(4) and, next, by assuming independent variations of the unknown functions $((U_\alpha, w, \gamma_\alpha, \phi_A); \alpha \in \{1, 2\}, A \in \{0, 1, 2, 3\})$. After straightforward algebra, the Hamiltonian's principle can be put in the sum of integrals

$$\int_{t_1}^{t_2} (\delta K - \delta U + \delta W_1 + \delta W_2) \mathrm{d}t = 0 \ . \tag{15}$$

The first part holds for the kinetic energy that we do not write down here, since we deal only with static processes in the following. The second term in Eq. (15) is the variation of the internal force work, defined on the middle plane surface Σ of the plate

$$\begin{aligned} \delta U = \int_\Sigma \Big\{ & N_{\alpha\beta}(\delta U_\alpha)_{,\beta} - M_{\alpha\beta}(\delta w)_{,\alpha\beta} + \hat{M}_{\alpha\beta}(\delta\gamma_\alpha)_{,\beta} + \hat{Q}_\alpha \delta\gamma_\alpha + D_\alpha^{(0)}(\delta\phi_0)_{,\alpha} + D_\alpha^{(1)}(\delta\phi_1)_{,\alpha} \\ & + D_\alpha^{(2)}(\delta\phi_2)_{,\alpha} + D_\alpha^{(3)}(\delta\phi_3)_{,\alpha} + D_3^{(1)}\delta\phi_1 + D_3^{(2)}\delta\phi_2 + D_3^{(3)}\delta\phi_3 \Big\} \mathrm{d}S \ . \end{aligned} \tag{16}$$

Here, the generalized stresses and electric inductions are computed using the three-dimensional stresses σ_{ij} and electric displacement D_i

$$\left(N_{\alpha\beta}, M_{\alpha\beta}, \hat{M}_{\alpha\beta}\right) = \int_{-h/2}^{+h/2} (1, z, f(z)) \sigma_{\alpha\beta} \, \mathrm{d}z \ , \tag{17}$$

$$\hat{Q}_\alpha = \int_{-h/2}^{+h/2} f'(z) \sigma_{\alpha 3} \, \mathrm{d}z \ , \tag{18}$$

$$\left(D_\alpha^{(0)}, D_\alpha^{(1)}, D_\alpha^{(2)}, D_\alpha^{(3)}\right) = \int_{-h/2}^{+h/2} (1, z, P(z), g(z)) D_\alpha \, \mathrm{d}z \ , \tag{19}$$

$$\left(D_3^{(1)}, D_3^{(2)}, D_3^{(3)}\right) = \int_{-h/2}^{+h/2} (1, P'(z), g'(z)) D_3 \, \mathrm{d}z \ , \tag{20}$$

with $\alpha, \beta \in \{1, 2\}$ and prime $'$ denoting the derivative.

The last two terms in Eq. (15) denote the variational work of the applied force densities and electric charges applied on the upper and lower faces of the plate, as well as those applied to the lateral boundary of the plate. These variational works take on the form

$$\delta W_1 = \int_\Sigma (f_\alpha \delta U_\alpha - p\delta w + \hat{m}_\alpha \delta\gamma_\alpha + q_1 \delta\phi_1) \mathrm{d}S \ , \tag{21}$$

$$\delta W_2 = \int_{\mathscr{C}} \left(F_\alpha \delta U_\alpha + T\delta w + C_\alpha \delta\gamma_\alpha - M_f (\delta w)_{,n}\right) \mathrm{d}\ell - \sum_p Z_p \delta w_p \ . \tag{22}$$

Here, f_α and p are the surface force densities, $\hat{m}_\alpha$ is a surface moment density and q_1 is the surface electric charge density. In Eq. (22), F_α and T are linear force densities, M_f and C_α are linear torque densities defined along the plate contour, Z_p are transverse forces at the angular points of the edge boundary $\mathscr{C}$ of the plate, $\mathbf{n}$ is the unit normal to $\mathscr{C}$. It has been assumed that there is no electric charge on the lateral plate boundary, because the dielectric constant of the piezoelectric material is much larger than the dielectric constant of the surrounding air for electric fields of the same order.

Let's remark that in Eq. (21), concerning the applied electromechanical loads on the plate faces, the electric charge density q_1 is considered only because other generalized electric charges associated with the electric potential variations $\delta\phi_0$, $\delta\phi_2$ and $\delta\phi_3$ disappear. Indeed, these generalized electric charges can be connected with the electric boundary conditions on the top and bottom faces through the integration over the plate thickness as follows:

$$(q_0, q_1, q_2, q_3) = [(1, z, P(z), g(z)) D_3]_{-h/2}^{+h/2} \ .$$

Owing to $P(\pm h/2) = g(\pm h/2) = 0$ and the boundary conditions (14), q_1 is the only nonvanishing electric charge.

Using the variational calculus arguments, Eq. (15) along with the variations (16), (21) and (22) must be satisfied for arbitrary variations $(\delta U_\alpha, \delta w, \delta\gamma_\alpha, \delta\phi_A)$; $\alpha \in \{1, 2\}$, $A \in \{0, 1, 2, 3\}$. After some cumbersome but straightforward computations, we arrive (static case) at

$$N_{\alpha\beta,\beta} + f_\alpha = 0, \quad M_{\alpha\beta,\alpha\beta} - p = 0, \quad \hat{M}_{\alpha\beta,\beta} - \hat{Q}_\alpha + \hat{m}_\alpha = 0 \ , \tag{23}$$

and

$$D^{(0)}_{\alpha,\alpha} = 0, \ \ D^{(1)}_{\alpha,\alpha} - D^{(1)}_3 + q_1 = 0, \ \ D^{(2)}_{\alpha,\alpha} - D^{(2)}_3 = 0, \ \ D^{(3)}_{\alpha,\alpha} - D^{(3)}_3 = 0 \ . \tag{24}$$

The associated boundary conditions on the lateral plate contour $\mathscr{C}$ are

$$\begin{aligned}
&F_\alpha = N_{\alpha\beta} n_\beta \quad \text{or} \quad U_\alpha \text{ given}, \\
&T = \left(\tau_\alpha M_{\alpha\beta} n_\beta\right)_{,s} + n_\alpha M_{\alpha\beta,\beta} \quad \text{or} \quad w \text{ given}, \\
&M_f = n_\alpha M_{\alpha\beta} n_\beta \quad \text{or} \quad w_{,n} \text{ given}, \\
&C_\alpha = \hat{M}_{\alpha\beta} n_\beta \quad \text{or} \quad \gamma_\alpha \text{ given}, \\
&D^{(A)}_\alpha n_\alpha = 0 \quad (A \in \{0, 1, 2, 3\}) \quad \text{or} \quad \phi_A \text{ given} \ .
\end{aligned} \tag{25}$$

The vector $\boldsymbol{\tau}$ is the unit tangent vector to $\mathscr{C}$ and s is the curvilinear coordinate along the contour $\mathscr{C}$. In addition to Eq. (25), we have $[\![\tau_\alpha M_{\alpha\beta} n_\beta - Z_p]\!]_{A_p} = 0$, the condition at the angular points of the contour. The last equation of Eq. (25) are the boundary conditions along $\mathscr{C}$ associated with the electric quantities. In addition, the right-hand side of $(25)_5$ is zero, according to the above remarks. There is no electric charge and no electrode on the lateral surface of the plate.

The first two equations in Eq. (23) are similar to those of the Love-Kirchhoff first-order theory of thin plates, and the third equation represents the equation of the shearing effects. The set of Eqs. (24) is, in fact, deduced from the conservation of the electric charge or the Gauss equation. These equations govern the generalized electric displacements or electric charges associated with the electric potential functions $\phi_A (A \in \{0, 1, 2, 3\})$ introduced in the third equation of the expansion (10). In the second equation of (24), we note the generalized electric charge due to the surface density of electric charge applied to the top and bottom faces of the plate.

In the case of an electric potential applied to the top and bottom faces of the plate, the functions ϕ_0 and ϕ_1 are no longer unknown, but they are related to the applied electric potential through (13). Therefore, the first two equations of Eq. (24) do not appear, and the number of unknown functions as well as the equations are then reduced in this situation.

5 The plate constitutive laws

A. Applied electric charges

We restrict the study to constitutive laws for linear piezoelectricity, see Eqs. (9), of materials with orthotropic symmetry, [12, 20]. To this end, we compute the generalized stress and electric inductions resultants defined by Eqs. (17)–(20), by using the constitutive laws (9). The results can be put in the matrix form

$$\begin{bmatrix} N_1 \\ N_2 \\ N_6 \\ D_3^{(1)} \end{bmatrix} = \begin{bmatrix} Q_{11} & Q_{12} & 0 & a_{31} \\ Q_{12} & Q_{22} & 0 & a_{32} \\ 0 & 0 & Q_{66} & 0 \\ a_{31} & a_{32} & 0 & f_{33} \end{bmatrix} \begin{bmatrix} S_1^{(0)} \\ S_2^{(0)} \\ S_6^{(0)} \\ \phi_1 \end{bmatrix} . \tag{26}$$

The other constitutive laws take on the matrix form too:

$$\begin{bmatrix} M_1 \\ M_2 \\ M_6 \\ \hat{M}_1 \\ \hat{M}_2 \\ \hat{M}_6 \\ D_3^{(2)} \\ D_3^{(3)} \end{bmatrix} = \begin{bmatrix} D_{11} & D_{12} & 0 & d_{11} & d_{12} & 0 & R_{31} & r_{31} \\ & D_{22} & 0 & d_{12} & d_{22} & 0 & R_{32} & r_{32} \\ & & D_{66} & 0 & 0 & d_{66} & 0 & 0 \\ & & & \hat{D}_{11} & \hat{D}_{12} & 0 & \hat{R}_{31} & \hat{r}_{31} \\ & & & & \hat{D}_{22} & 0 & \hat{R}_{32} & \hat{r}_{32} \\ & & \text{(sym.)} & & & \hat{D}_{66} & 0 & 0 \\ & & & & & & P_{33} & \bar{P}_{33} \\ & & & & & & & \bar{\bar{P}}_{33} \end{bmatrix} \begin{bmatrix} S_1^{(1)} \\ S_2^{(1)} \\ S_6^{(1)} \\ S_1^{(2)} \\ S_2^{(2)} \\ S_6^{(2)} \\ \phi_2 \\ \phi_3 \end{bmatrix} . \tag{27}$$

The shear and electric induction resultants are

$$\begin{bmatrix} \hat{Q}_1 \\ \hat{Q}_2 \\ D_1^{(0)} \\ D_2^{(0)} \\ D_1^{(2)} \\ D_2^{(2)} \\ D_1^{(3)} \\ D_2^{(3)} \end{bmatrix} = \begin{bmatrix} \hat{A}_{55} & 0 & l_{15} & 0 & L_{15} & 0 & \bar{L}_{15} & 0 \\ & \hat{A}_{44} & 0 & l_{24} & 0 & L_{24} & 0 & \bar{L}_{24} \\ & & f_{11} & 0 & F_{11} & 0 & \bar{F}_{11} & 0 \\ & & & f_{22} & 0 & F_{22} & 0 & \bar{F}_{22} \\ & & & & B_{11} & 0 & \bar{B}_{11} & 0 \\ & \text{(sym.)} & & & & B_{22} & 0 & \bar{B}_{22} \\ & & & & & & \bar{\bar{B}}_{11} & 0 \\ & & & & & & & \bar{\bar{B}}_{22} \end{bmatrix} \begin{bmatrix} \gamma_1 \\ \gamma_2 \\ \phi_{0,1} \\ \phi_{0,2} \\ \phi_{2,1} \\ \phi_{2,2} \\ \phi_{3,1} \\ \phi_{3,2} \end{bmatrix} . \tag{28}$$

At last, we have as well

$$\begin{bmatrix} D_1^{(1)} \\ D_2^{(1)} \end{bmatrix} = \begin{bmatrix} b_{11} & 0 \\ 0 & b_{22} \end{bmatrix} \begin{bmatrix} \phi_{1,1} \\ \phi_{1,2} \end{bmatrix} . \tag{29}$$

All the coefficients introduced in the matrices are defined in Appendix A. These coefficients depend on the material constants of the piezoelectric plate and its thickness.

The strain tensors, which has been introduced in the constitutive laws (26)–(27), are defined from Eq. (10) by

$$S^{(0)}_{\alpha\beta} = U_{(\alpha,\beta)}, \quad S^{(1)}_{\alpha\beta} = -w_{,\alpha\beta}, \quad S^{(2)}_{\alpha\beta} = \gamma_{(\alpha,\beta)} \ . \tag{30}$$

It is worthwhile observing that we have electromechanical couplings between some generalized stress and electric induction resultants.

B. Applied electric potential

In the case of an applied electric potential, the functions ϕ_0 and ϕ_1 in the approximation (10) are no longer arbitrary and are given by $\phi_0 = 0$ and $\phi_1 = 2V/h$. Consequently, the constitutive law defined by Eq. (26) must be replaced by

$$\begin{bmatrix} N_1 \\ N_2 \\ N_6 \end{bmatrix} = \begin{bmatrix} Q_{11} & Q_{12} & 0 \\ Q_{12} & Q_{22} & 0 \\ 0 & 0 & Q_{66} \end{bmatrix} \begin{bmatrix} S^{(0)}_1 \\ S^{(0)}_2 \\ S^{(0)}_6 \end{bmatrix} + \begin{bmatrix} e^*_{31} \\ e^*_{32} \\ 0 \end{bmatrix} 2V \ . \tag{31}$$

The effective piezoelectric constants e^*_{31} and e^*_{32} are given in Appendix A. The constitutive law (27) remains unchanged. However, in Eq. (28), the rows and columns corresponding to the function ϕ_0 disappear, and the matrix in Eq. (28) is of the 6×6 order; in addition, Eq. (29) is not considered. We note that according to Eq. (31), if an electric potential is applied on the top and bottom faces of the plate, only an elongation or compression of the plate will be produced.

6
Piezoelectric plate in cylindrical bending

Now, we intend to solve the problem of a piezoelectric plate undergoing applied surface force density, surface electric charge or electric potential in the *cylindrical bending* configuration, i.e. all the stresses, strains, displacements, electric field and potential do not depend on the y variable. Displacement u_2 plays no role in the problem; it can be cancelled out and we set $u_2 = 0$, $\gamma_2 = 0$. The shear traction is zero on the plate faces, $f_\alpha = 0$, and there is no surface moment density, $\hat{m}_\alpha = 0$. The *simple support conditions* for a rectangular plate of length L are given by (see Fig. 1)

$$\sigma_{11}(0,z) = \sigma_{11}(L,z) = 0, \quad \sigma_{13}(0,z) = \sigma_{13}(L,z) = 0, \quad u_3(0,z) = u_3(L,z) = 0 \ . \tag{32}$$

It is noticed that the boundary conditions along the contour $\mathscr{C}$ are obviously satisfied in the cylindrical bending configuration.

With a view toward satisfying the boundary conditions (32), the load functions are expanded in a Fourier series over the segment $[0, L]$. Consequently, the surface density of force, surface

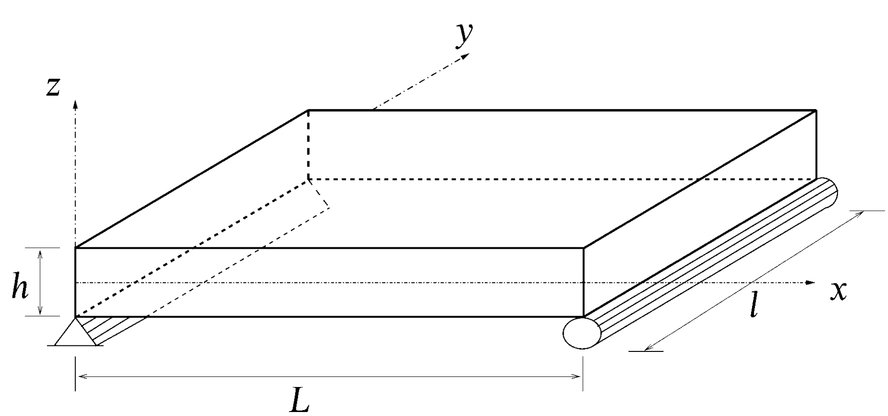

Fig. 1. Piezoelectric plate on simple supports

density of electric charge and electric potential applied to the plate faces can be expressed in the form

$$(p(x), Q(x), V(x)) = \sum_{n=1}^{\infty} (S_n, Q_n, V_n) \sin \lambda_n x \ , \tag{33}$$

with

$$\lambda_n = \frac{n\pi}{L}, \quad (S_n, Q_n, V_n) = \frac{4}{n\pi}(S_0, Q_0, V_0) \ . \tag{34}$$

Loads defined by the above equations represent uniform applied surface density of force S_0, density of electric charge Q_0 and electric potential V_0, respectively. Because of the load functions (33) and the boundary conditions (32), it is natural to search for a solution to the plate problem given by Eqs. (23)–(24), along with the constitutive laws (26)–(29), also as Fourier series as follows:

$$\begin{aligned} (U_1(x), \gamma_1(x)) &= \sum_{n=1}^{\infty} (U_n, \Gamma_n) \cos \lambda_n x, \\ (w(x), \phi_0(x), \phi_1(x), \phi_2(x), \phi_3(x)) &= \sum_{n=1}^{\infty} \left(W_n, \Phi_{0,n}, \Phi_{1,n}, \Phi_{2,n}, \Phi_{3,n}\right) \sin \lambda_n x \ . \end{aligned} \tag{35}$$

We recall that, in the case of an applied electric potential, the number of unknown functions is reduced; especially, ϕ_0 and ϕ_1 are not accounted for. In this situation, the applied electric charge $Q(x)$ is not considered as a load.

Now, we have all the ingredients in view of solving the cylindrical bending of a simply supported piezoelectric plate. The Fourier coefficients in the series (35) are determined by first substituting the solution (35) into the constitutive laws (26)–(29) and the results into the plate equations (23)–(24). The Fourier coefficients are then the solution to a set of linear algebraic equations for each n, which can be written in matrix form.

A. Applied surface density of force and/or electric charge

The set of linear equations for the Fourier coefficients takes on the form

$$A_n^Q X_n^Q = B_n^Q \ , \tag{36}$$

with the matrix and vectors

$$A_n^Q = \begin{bmatrix} -\lambda_n^2 C_{11}^* & 0 & 0 & 0 & \lambda_n e_{31}^* & 0 & 0 \\ & -\frac{\lambda_n^4}{12} C_{11}^* & \frac{\lambda_n^3}{\pi^3} C_{11}^* & 0 & 0 & -\frac{\lambda_n^2}{6} e_{31}^* & \frac{2\lambda_n^2}{\pi^2} e_{31}^* \\ & & -\frac{1}{2}\left(C_{55}^* + \frac{\lambda_n^2}{\pi^2} C_{11}^*\right) & \frac{2\lambda_n}{\pi} e_{15}^* & 0 & \frac{4\lambda_n}{\pi^3}\left(e_{31}^* + e_{15}^*\right) & -\frac{\lambda_n}{2\pi}\left(e_{31}^* + e_{15}^*\right) \\ & & & \lambda_n^2 \epsilon_{11}^* & 0 & -\frac{\lambda_n^2}{6} \epsilon_{11}^* & \frac{2\lambda_n^2}{\pi^2} \epsilon_{11}^* \\ & & & & \epsilon_{33}^* + \frac{\lambda_n^2}{12} \epsilon_{11}^* & 0 & 0 \\ & & \text{(sym.)} & & & \frac{1}{3}\left(\epsilon_{33}^* + \frac{\lambda_n^2}{10} \epsilon_{11}^*\right) & -\frac{4}{\pi^2}\left(\epsilon_{33}^* + \frac{\lambda_n^2}{\pi^2} \epsilon_{11}^*\right) \\ & & & & & & \frac{1}{2}\left(\epsilon_{33}^* + \frac{\lambda_n^2}{\pi^2} \epsilon_{11}^*\right) \end{bmatrix},$$

$$[X_n^Q]^T = \left(U_n, W_n, \Gamma_n, \Phi_{0,n}, \Phi_{1,n}, \Phi_{2,n}, \Phi_{3,n}\right),$$

$$[B_n^Q]^T = (0, S_n, 0, 0, -Q_n, 0, 0) \ .$$

B. Applied surface density of force and/or electric potential

In this case, the set of linear algebraic equations is simpler since the number of equations is reduced

$$A_n^V X_n^V = B_n^V \ , \tag{37}$$

with the matrix and vectors

$$A_n^V = \begin{bmatrix} -\lambda_n^2 C_{11}^* & 0 & 0 & 0 & 0 \\ & -\frac{\lambda_n^4}{12} C_{11}^* & \frac{\lambda_n^3}{\pi^3} C_{11}^* & -\frac{\lambda_n^2}{6} e_{31}^* & \frac{2\lambda_n^2}{\pi^2} e_{31}^* \\ & & -\frac{1}{2}\left(C_{55}^* + \frac{\lambda_n^2}{\pi^2} C_{11}^*\right) & \frac{4\lambda_n}{\pi^3}\left(e_{31}^* + e_{15}^*\right) & -\frac{\lambda_n}{2\pi}\left(e_{31}^* + e_{15}^*\right) \\ & \text{(sym.)} & & \frac{1}{3}\left(\epsilon_{33}^* + \frac{\lambda_n^2}{10}\epsilon_{11}^*\right) & -\frac{4}{\pi^2}\left(\epsilon_{33}^* + \frac{\lambda_n^2}{\pi^2}\epsilon_{11}^*\right) \\ & & & & \frac{1}{2}\left(\epsilon_{33}^* + \frac{\lambda_n^2}{\pi^2}\epsilon_{11}^*\right) \end{bmatrix},$$

$$[X_n^V]^T = \left(U_n, W_n, \Gamma_n, \Phi_{2,n}, \Phi_{3,n}\right),$$

$$[B_n^V]^T = \left(-2\lambda_n e_{31}^* V_n, S_n, 0, 0, 0\right) \ .$$

In both cases, the matrices consist of real elements and are symmetric. Now the way of solving the plate problem is straightforward: first solve Eq. (36) or (37), to find the Fourier coefficients, then substitute the results into the Fourier series (35), go back to the displacement field and electric potential by means of Eq. (10). Afterward, the stresses and electric displacement are computed through the constitutive laws of linear piezoelectricity specialized for orthotropic materials.

7 Numerical investigations and comparisons

Numerical simulations of the present plate model are considered for a single plate made of PZT-4 ceramics whose nonzero material constants are listed in Table 1, [20]. The geometry of the plate is $h = 0.001$ m and two slenderness ratios $L/h = 10$ and $L/h = 50$ are considered. The numerical results for the mechanical and electric quantities are given with the following dimensionless units:

(i) for the surface density of the normal force $S_0 \neq 0 (S_0 = 1000 \ \ \mathrm{N/m^2})$, we set

$$(U, W, \Phi) = \frac{C_{11}^E}{hS_0}\left(u_1, u_3, \frac{\phi}{E_0}\right), \quad \left(T_{ij}, \mathscr{D}_l\right) = \frac{1}{S_0}\left(\sigma_{ij}, E_0 D_l\right) \ ,$$

(ii) for the surface density of the electric charge $Q_0 \neq 0 (Q_0 = 10 \ \mathrm{C/m^2})$, we set

$$(U, W, \Phi) = \frac{C_{11}^E}{hE_0 Q_0}\left(u_1, u_3, \frac{\phi}{E_0}\right), \quad \left(T_{ij}, \mathscr{D}_l\right) = \frac{1}{E_0 Q_0}\left(\sigma_{ij}, E_0 D_l\right) \ ,$$

(iii) for the applied electric potential $V_0 \neq 0 (V_0 = 50 \ \mathrm{V})$, we have

$$(U, W, \Phi) = \frac{E_0}{V_0}\left(u_1, u_3, \frac{\phi}{E_0}\right), \quad \left(T_{ij}, \mathscr{D}_l\right) = \frac{hE_0}{C_{11}^E V_0}\left(\sigma_{ij}, E_0 D_l\right) \ .$$

For the numerical simulations, we take $E_0 = 10^{10}$ V/m. The number of terms retained in series (35) are adjusted according to the slenderness ratios and electromechanical loads, then considered in order to ensure the convergence. The finite element (FE) computations for

Table 1. Independent elastic, piezoelectric and dielectric constants of a piezoelectric material (transversely isotropic symmetry)

	C_{11}^E (GPa)	C_{12}^E	C_{33}^E	C_{13}^E	C_{44}^E	e_{31} ($\mathrm{C/m^2}$)	e_{33}	e_{15}	ϵ_{11} (nF/m)	ϵ_{33}
PZT-4	139.0	77.8	115.0	74.3	25.6	−5.2	15.1	12.7	13.06	11.51

comparison are performed with ABAQUS code by using plane strain elements of 8-node bi-quadratic type and 800 elements are considered for both $L/h = 10$ and $L/h = 50$.

Case 1a. Surface density of normal force applied to the top face of the plate, closed circuit
It means that $V_0 = 0$. In the present situation, only the set of linear algebraic equations (37) is considered. The through-thickness distributions for U, W, Φ and T_{11} are presented in Fig. 2 for the ratio $L/h = 10$. The displacement U at $x = 0$ is plotted in Fig. 2a, and it is almost linear through the plate thickness. The flexural displacement W at $x = L/2$ is given in Fig. 2b, the straight line corresponds to the present plate approach, while the small circles are the FE computations and the straight dashed-line is the result provided by the classical thin plate theory based on the Love's assumption (no shear correction, that is, $f(z) = 0$ and $g(z) = 0$ in Eq. (10)). We observe that the discrepancy between the maximum values of the deflection (at $z = 0$) for the 3D computation and that of the plate model is <0.02%, however, the difference becomes bigger, about 3%, for the classical thin plate model. The most interesting result is the electric potential at $x = L/2$ plotted in Fig. 2c. The electric potential is, in fact, induced by the elastic deformation through the piezoelectric coupling. We first note a very good accuracy with the finite element method (FEM). Next, the result ascertains the existence of the ϕ_2 term in the electric potential approximation (10). However, if the ϕ_2 term is absent from the expansion (10), there is no induced electric potential through the plate thickness. The shear stress T_{13} at $x = L/4$ is drawn in Fig. 2d. The identical simulations are performed with the slenderness ratio $L/h = 50$, and the results are presented in Fig. 3 for the same electromechanical quantities as in the previous figure. The difference between the results coming from the plate model and those of the FE simulations are very small since we are closer to the thin plate assumption. Especially the discrepancy between the maxima of the deflection displacement at the plate center for the present plate model and FE results is now <0.01%, whereas this difference is about 0.1% for the classical plate theory. Going back to the physical units, we have an estimate of 9 μm for the deflection at the plate center and the maximum of the induced electric potential is about 4.8 V for the slenderness ratio $L/h = 50$.

Case 1b. Surface density of normal force applied to the top face of the plate, open circuit
In this situation, the algebraic equations are given by Eq. (36) with $S_0 \neq 0$ and $Q_0 = 0$. The electromechanical response of the piezoelectric plate is shown in Fig. 4 for the profiles of

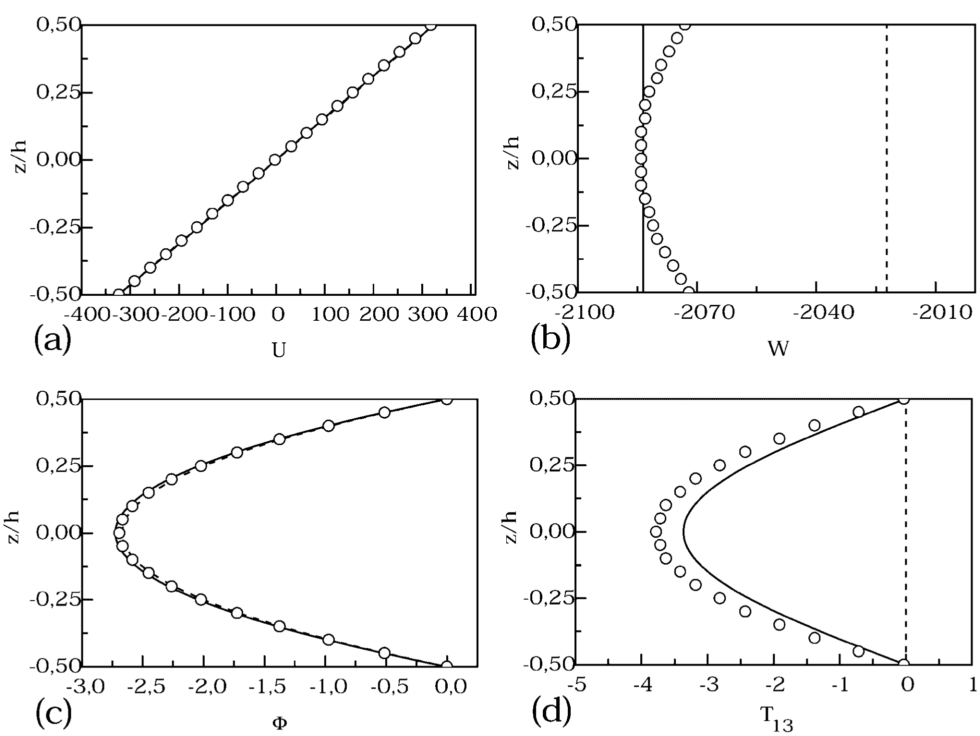

Fig. 2. Force density applied on the top face of a piezoelectric single plate in closed circuit for $L/h = 10$. Plate model (full line), finite element (small circles) and simplified plate model (dashed-line)

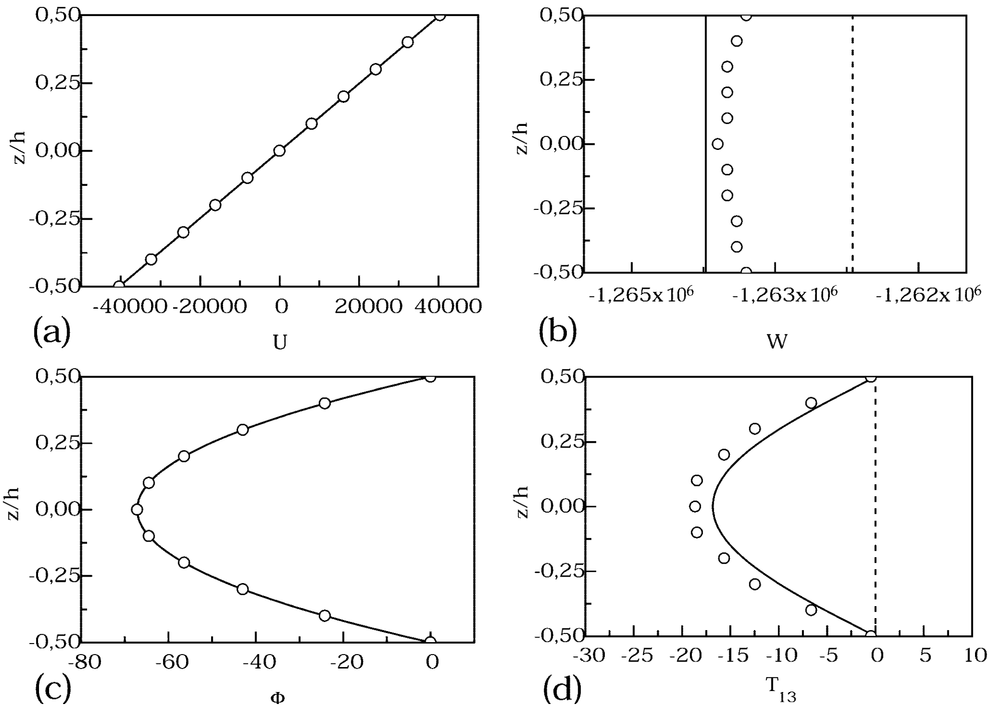

Fig. 3. Force density applied on the top face of a piezoelectric single plate in closed circuit for $L/h = 50$. Plate model (full line), finite element (small circles) and simplified plate model (dashed-line)

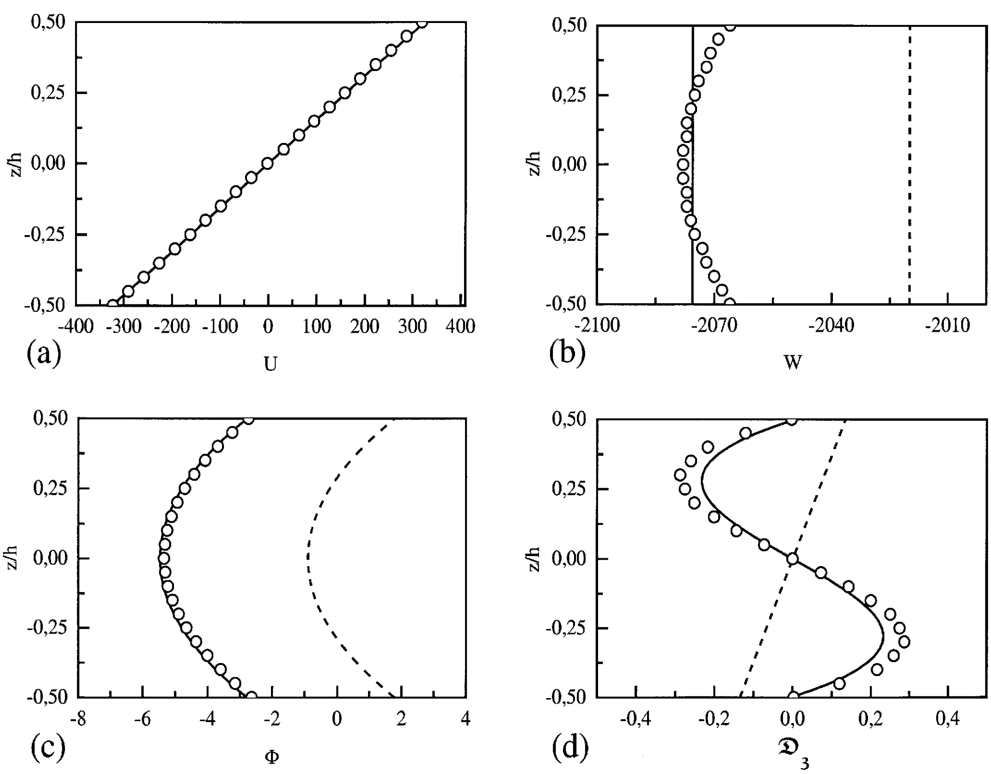

Fig. 4. Force density applied on the top face of a piezoelectric single plate in open circuit for $L/h = 10$. Plate model (full line), finite element (small circles) and simplified plate model (dashed-line)

U, W, Φ and $\mathscr{D}_3$ as functions of the thickness coordinate for the thickness aspect ratio $L/h = 10$. Figure 4a presents the displacement U at $x = 0$. The deflection W at $x = L/2$ is given in Fig. 4b. The difference between maxima of the deflection at the plate center for the present plate approach (straight line) and FE simulation (small circles) is evaluated at 0.1%, whereas the same comparison to the simplified plate theory (dashed-line curve) yields an error of 2.8%. The induced electric potential at $x = L/2$ is plotted in Fig. 4c and the potential variation possesses a parabolic profile. Finally, Fig. 4d shows the normal component of the electric displacement or induction $\mathscr{D}_3$ at $x = L/2$. The comparison of the latter electrical quantity particularly speaks for itself. Indeed, we have an excellent agreement with the FE results, whereas the classical thin plate theory (dashed-line curve) does not give the correct through-the-thickness profile. Similar results are presented in Fig. 5 for the same quantities with the slenderness ratio $L/h = 50$. The present plate model gives accurate predictions for the different electromechanical variables, displacements, stresses, electric potential and displacement. Especially, the estimate error between the deflection at the plate center for the FEM and our improved plate model is about 0.01% and 0.1% for the simplified thin plate approach. The comparison between the results provided by the FEM and those coming from the present model illustrates the performance of the plate model and gives very good predictions with minor differences. The comparison made with the classical thin plate theory (no shear effect) ascertains the efficiency of our plate modelling.

Case 2. Applied electric potential

In this situation, the set of linear algebraic equations (37) is solved with $V_0 \neq 0$ and $S_0 = 0$. The results are collected together in Table 2 in dimensionless units for the displacement U at $x = L$, stress T_{22} at the plate center and the normal component of the electric displacement for two slenderness ratios $L/h = 10$ and $L/h = 50$. Only an elongational deformation along the x-axis is obviously produced, and, in this case, the shear effect does not play any role. A comparison is done with the FE computations and the plate model, providing rather quite good estimates. We note that the thickness aspect ratio has obviously no influence on the stress T_{22} and the electric displacement component $\mathscr{D}_3$. In addition, the electric potential is linear through the plate thickness going from $-V$ at $z = -h/2$ to $+V$ at $z = +h/2$. The elongation of the plate produced by the applied electric potential is about 0.4 μm for the ratio $L/h = 50$.

Case 3. Applied electric charges

For this case, we solve the set of linear algebraic equations (36) with $S_0 = 0$ and $Q_0 \neq 0$. As in the problem of an applied electric potential, only elongational deformation is obtained. Table 3

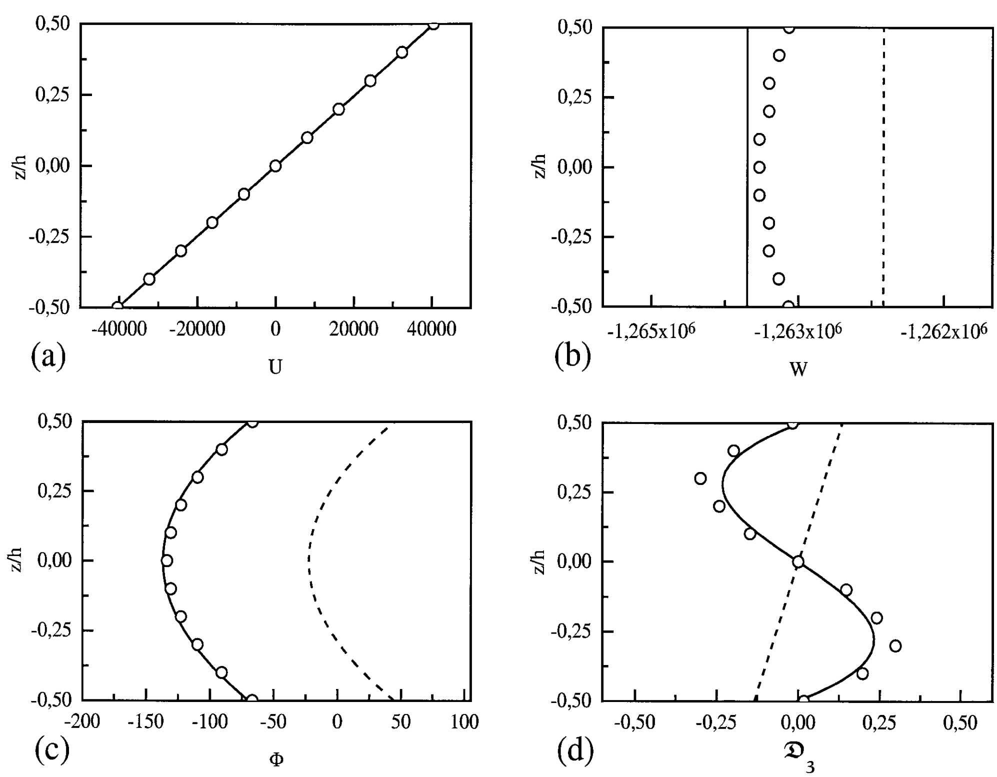

Fig. 5. Force density applied on the top face of a piezoelectric single plate in open circuit for $L/h = 50$. Plate model (full line), finite element (small circles) and simplified plate model (dashed-line)

Table 2. Single piezoelectric plate, applied electric potential

	$L/h = 10$			$L/h = 50$		
	Plate model	Finite elements	Error (%)	Plate model	Finite elements	Error (%)
U at $x = L$	16.41	16.42	0.05	82.06	82.11	0.06
T_{22} at $x = L/2$	−1.447	−1.446	0.09	−1.447	−1.446	0.09
$\mathscr{D}_3$ at $x = L/2$	−22.96	−22.94	0.08	−22.96	−22.94	0.08

Table 3. Single piezoelectric plate, applied electric charges

	$L/h = 10$			$L/h = 50$		
	Plate model	Finite elements	Error (%)	Plate model	Finite elements	Error (%)
U at $x = L$	0.6785	0.716	5.2	3.54	3.58	1.0
T_{22} at $x = L/2$	0.063043	0.063044	0.001	0.063043	0.063044	0.001
Φ at $x = L/2$	0.043597	0.0436	0.007	0.043597	0.0436	0.007

gives the essential numerical results in dimensionless units for U, T_{22} and the electric potential Φ for two characteristic thickness aspect ratios $L/h = 10$ and $L/h = 50$. The comparison with the FEM performed on the 3D problem shows a rather good accuracy of the present plate model, except for the elongational displacement. As in the case of an applied electric potential, the shear effect is obviouly zero and there is no difference with the simplified model (Love-Kirchhoff approach).

In the case of an applied electric potential or charges on the plate faces, a thickness deformation is obviously produced for the real 3D plate. Such a thickness variation is not accounted for in the present approach, since the deflection displacement w is constant through the plate thickness, which explains the small discrepancy observed in the cases 2 and 3. In spite of this limitation, the thickness variation represents, however, $<1\%$ of the elongation or compression in the direction of the plate length.

Additional comparisons can be done to exact solutions for laminated piezoelectric plates in cylindrical bending, which are merely an extension of the work for elastic laminates, [21], to piezoelectric plates, [22].

8
Closing remarks and future directions

In the present work, we attempt to promote an efficient and interesting approach to piezoelectric plates. The field approximation accounts for the shear effects modelled by a sine function and a refined electric potential distribution through the plate thickness. First, some comparative tests between our improved plate model and the FE computations and, next, the classical thin plate theory allow us to ascertain the validity and the capability of the piezoelectric plate model considered. Especially benchmark tests carried out for different kinds of electromechanical loads: (i) normal force at the top surface of the plate, (ii) electric potential at the top and bottom faces of the plate, and (iii) electric charges on both faces of the plate show the advantages of the model. In the case of an applied normal force density for an open and closed circuits, the through-thickness distributions of the most pertinent electromechanical variables have been computed for the present model, and compared with the FE computations for the 3D plate and with the simplified plate model. The comparisons yield an excellent agreement of the present model with the FEM. The approach to piezolectric plates provides very accurate predictions (error $<0.1\%$ for the deflection displacement), whereas the classical thin plate theory gives less accurate results. It should be underlined (i) *the influence of the shear correction* described by a sine function on the computation of the *shear stress through the plate thickness*, (ii) the *accurate approximation of the electric potential* (see the third expansion in Eq. (10)), giving rise to the induced electric potential, and (iii) the use of the *approximate charge equation* for the generalized electric charges or inductions (see Eq. (24)), which avoids assuming a constant electric displacement through the plate thickness.

An important extension of the present work concerns laminated piezoelectric plates, that is, plates made of piezoelectric and purely elastic layers. In view of the results for the single-layered plate, we are encouraged to study the vibrations of laminated piezoelectric plates [23–26], which is particularly usefull for active or passive control of vibrations. At last, the edge effects, such as electric field concentration, can be interesting to investigate, especially for plates partly coated with piezoelectric slabs.

Appendix A

All coefficients introduced in the matrices (26)–(29) are defined by

$$\left(Q_{ab}, D_{ab}, d_{ab}, \hat{D}_{ab}\right) = \left(1, \frac{h^2}{12}, \frac{2h^2}{\pi^3}, \frac{h^3}{2\pi^2}\right) h C^*_{ab} \ ,$$

$$\hat{A}_{MN} = \frac{h}{2} C^*_{MN} \ ,$$

$$\left(a_{2\alpha}, R_{3\alpha}, r_{3\alpha}, \hat{R}_{3\alpha}, \hat{r}_{3\alpha}\right) = \left(1, \frac{h^2}{6}, -\frac{2h}{\pi^2}, \frac{4h^3}{\pi^3}, -\frac{h}{2\pi}\right) h e^*_{3\alpha} \ ,$$

$$\left(l_{\alpha N}, L_{\alpha N}, \bar{L}_{\alpha N}\right) = \left(\frac{2}{\pi}, -\frac{4h^2}{\pi^3}, \frac{h}{2\pi}\right) h e^*_{\alpha N} \ ,$$

$$\left(b_{\alpha\alpha}, B_{\alpha\alpha}, \bar{B}_{\alpha\alpha}, \bar{\bar{B}}_{\alpha\alpha}, f_{\alpha\alpha}, F_{\alpha\alpha}, \bar{F}_{\alpha\alpha}\right) = \left(-\frac{h^2}{12}, -\frac{h^4}{30}, \frac{4h^3}{\pi^4}, -\frac{h^2}{2\pi^2}, -1, \frac{h^2}{6}, -\frac{2h}{\pi^2}\right) h \epsilon^*_{\alpha\alpha} \ ,$$

$$\left(f_{33}, P_{33}, \bar{P}_{33}, \bar{\bar{P}}_{33}\right) = \left(-1, -\frac{h^2}{3}, \frac{4h}{\pi^2}, -\frac{1}{2}\right) h \epsilon^*_{33} \ ,$$

with the definitions $(ab) \in \{(11), (22), (12), (66)\}$, $\alpha \in \{1, 2\}$, $(MN) \in \{(44), (55)\}$ and $(\alpha N) \in \{(24), (15)\}$ (the Voigt notation is used for convenience). The modulus of elasticity due to the normal shear stress hypothesis (σ_{33} negligible in comparison to the other stress components) are given by $C^*_{ab} = C^E_{ab} - C^E_{a3} C^E_{3b} / C^E_{33}$. On using the same argument, we have the effective piezoelectric and dielectric coefficients $e^*_{ja} = e_{ja} - e_{j3} C^E_{a3} / C^E_{33}$ and $\epsilon^*_{ij} = \epsilon_{ij} + e_{i3} e_{j3} / C^E_{33}$ (with $a \in \{1, ..., 6\}, \quad j \in \{1, 2, 3\}$).

References

1. **Sunar, M.; Rao, S.S.:** Recent advances in sensing and control of flexible structures via piezoelectric materials technology. Appl Mech Rev 52 (1999) 1–16
2. **Loewy, R.G.:** Recent developments in smart structures with aeronautical applications. Smart Mat Struct 6 (1997) R11–R42
3. **Hagoud, N.W.; Chung, W.H.; Von Flotow, A.:** Modelling of piezoelectric actuator dynamics for active structural control. J Intelligent Mat Syst Struct 1 (1990) 327–354
4. **Peters, D.J.; Blackford B.L.:** Piezoelectric bimorph-based translation device for two-dimensional, remote micropositioning. Rev Sci Instrum 60 (1989) 138–140
5. **Touratier, M.:** An efficient standard plate theory. Int J Eng Sci 29 (1991) 901–916
6. **Saravanos, D.A.; Heyliger, P.R.:** Mechanics and computational models for laminated piezoelectric beams, plates, and shells. Appl Mech Rev 52 (1999) 305–320
7. **Tiersten, H.F.:** Linear piezoelectric plate vibrations. New York: Plenum 1969
8. **Mindlin, R.D.:** High frequency vibrations of piezoelectric crystal plates. Int J Solids Struct 8 (1972) 895–906
9. **Lee, C.K.:** Theory of laminated piezoelectric plates for the design of distributed sensors/actuators. Part 1: Governing equations and reciprocal relationships. J Acoust Soc Am 87 (1990) 1144–1158
10. **Zhang, X.D.; Sun, C.T.:** Analysis of a sandwich plate containing a piezoelectric core. Smart Mat Struct 8 (1999) 31–40
11. **Rogacheva, N.N.:** The theory of piezoelectric shells and plates. Boca Raton: CRC Press 1994
12. **Ikeda, T.:** Fundamentals of piezoelectricity. Oxford: Oxford University Press 1996
13. **Maugin, G.A.; Attou, D.:** An asymptotic theory of thin piezoelectric plates. J Int Mech Appl Math 43 (1990) 347–362
14. **Love, A.E.H.:** Treatise on the mathematical theory of elasticity. New York: Dover 1944
15. **Reissner, E.:** On transverse bending of plates including the effect of transverse shear deformation. Int J Solids Struct 11 (1975) 569–573
16. **Ambartsunian, S.A.:** The theory of the anisotropic plates. Moscow: Nauka 1967

17. **Reddy, J.N.:** A simple higher-order theory for laminated composite plates. ASME J Appl Mech 51 (1984) 745–752
18. **Touratier, M.:** A refined theory of laminated shallow shells. Int J Solids Struct 29 (1992) 1401–1415
19. **Eringen, A.C.; Maugin, G.A.:** Electrodynamics of continua. I. Foundations and solid media. New York: Springer-Verlag 1990
20. **Berlincourt, D.A.; Curran, D.R.; Jaffe, H.:** Piezoelectric and piezomagnetic materials and their function in transducers. In: Mason, W.P. (ed.) Physical Acoustics I (1964) 169–270
21. **Pagano, N.J.:** Exact solutions for composite laminates in cylindrical bending. J Composite Mat 3 (1969) 398–411
22. **Heyliger, P.; Brooks, S.:** Exact solutions for laminated piezoelectric plates in cylindrical bending. ASME J Appl Mech 63 (1996) 903–910
23. **Carrera, E.:** An improved Reissner-Mindlin-type model for the electromechanical analysis of multilayered plates including piezo-layers. J Intelligent Mat Syst Struct 8 (1997) 232–248

24. **Mitchell, J.A.; Reddy, J.N.:** A refined hybrid plate theory for composite laminates with piezoelectric laminae. Int J Solids Struct 32 (1995) 2345–2367
25. **Heyliger, P.; Brooks, S.:** Free vibration of piezoelectric laminates in cylindrical bending. Int J Solids Struct 32 (1995) 2945–2960
26. **Yang, J.S.:** Equations for the extension and flexure of electroelastic plates under strong electric fields. Int J Solids Struct 36 (1999) 3171–3192